J Biosci Vol. 43, No. 4, September 2018, pp. 693–706
DOI: 10.1007/s12038-018-9794-x

© Indian Academy of Sciences

A putative *NEM1* homologue regulates lipid droplet biogenesis *via PAH1* in *Tetrahymena thermophila*

Sushmita Shukla, Anoop Narayana Pillai and Abdur Rahaman*

National Institute of Science Education and Research (NISER), Bhubaneswar, HBNI, P.O. Jatni, Khurda, Odisha 752 050, India

**Corresponding author (Email, arahaman@niser.ac.in)*

MS received 17 March 2018; accepted 19 June 2018; published online 16 August 2018

Nuclear envelope morphology protein 1 (*NEM1*) along with a phosphatidate phosphatase (*PAH1*) regulates lipid homeostasis and membrane biogenesis in yeast and mammals. We investigated four putative *NEM1* homologues (*TtNEM1A*, *TtNEM1B*, *TtNEM1C* and *TtNEM1D*) in the *Tetrahymena thermophila* genome. Disruption of *TtNEM1B*, *TtNEM1C* or *TtNEM1D* did not compromise normal cell growth. In contrast, we were unable to generate knockout strain of *TtNEM1A* under the same conditions, indicating that *TtNEM1A* is essential for *Tetrahymena* growth. Interestingly, loss of *TtNEM1B* but not *TtNEM1C* or *TtNEM1D* caused a reduction in lipid droplet number. Similar to yeast and mammals, TtNem1B of *Tetrahymena* exerts its function *via* Pah1, since we found that *PAH1* overexpression rescued loss of Nem1 function. However, unlike *NEM1* in other organisms, *TtNEM1B* does not regulate ER/nuclear morphology. Similarly, neither *TtNEM1C* nor *TtNEM1D* is required to maintain normal ER morphology. While *Tetrahymena PAH1* was shown to functionally replace yeast *PAH1* earlier, we observed that *Tetrahymena NEM1* homologues did not functionally replace yeast *NEM1*. Overall, our results suggest the presence of a conserved cascade for regulation of lipid homeostasis and membrane biogenesis in *Tetrahymena*. Our results also suggest a Nem1-independent function of Pah1 in the regulation of ER morphology in *Tetrahymena*.

Keywords. Endoplasmic reticulum; lipid droplet; membrane biogenesis; NEM1; phosphatidate phosphatase; *Tetrahymena thermophila*

1. Introduction

PAH/LIPIN plays a pivotal role in lipid metabolism by catalysing the Mg^{2+}-dependent dephosphorylation of phosphatidic acid (PA) to yield diacylglycerol (DAG), a fundamental reaction in lipid biosynthesis (Han *et al*. 2006; Han *et al*. 2007; Han and Carman 2010). DAG can be acylated by DAG acyltransferases (DGATs) to produce triacylglycerols (TAG), used for the synthesis *via* the Kennedy pathway of membrane phospholipids phosphatidylcholine (PC) and phosphatidylethanolamine (PE) (figure 1a) (Carman and Han 2009b; Siniossoglou 2009; Gibellini and Smith 2010; Pascual and Carman 2013). The activity of Pah1 is regulated by phosphorylation. Multiple kinases including protein kinase A, Pho85p–Pho80p and CDC28 (CDK1: cyclin-dependent kinase) function in a negative regulatory manner to phosphorylate Pah1 at multiple serine and threonine residues in a cell cycle-dependent fashion (Choi *et al*. 2012; Su *et al*. 2012; Su *et al*. 2014; Hsieh *et al*. 2016). Positive activation occurs *via* a highly conserved membrane-associated protein phosphatase complex comprising Nem1 (catalytic subunit) and Spo7 (regulatory subunit), which dephosphorylates and recruits Pah1 to the nuclear/ER membrane (figure 1b) (Siniossoglou *et al*. 1998; O'Hara *et al*. 2006; Kim *et al*. 2007). The dephosphorylation of Pah1 exclusively by Nem1–Spo7 acts as a rate-limiting step and is essential for its phosphatidate phosphatase function. Thus, this cascade is essential in the regulation of lipid metabolism and membrane biogenesis (Karanasios *et al*. 2010; Karanasios *et al*. 2013). Cells lacking either the Nem1 or Spo7 subunits of the complex mirror the phenotypes of *pah1*Δ cells including increased phospholipid synthesis, aberrant expansion of the nuclear/ER membrane, decreased lipid droplet number and growth inhibition (Carman and Han 2009a; Pascual and Carman 2013; Zhang and Reue 2017). The *nem1*Δ *spo7*Δ double mutants also show phenotypes similar to *pah1*Δ or *nem1*Δ or *spo7*Δ, suggesting that these three proteins work in unison (Siniossoglou *et al*. 1998; Santos-Rosa *et al*. 2005; Siniossoglou 2009). Overexpression of the Nem1–Spo7 phosphatase complex in yeast results in a lethal phenotype only in the presence of its substrate Pah1, indicating that an excess level of PAP activity is deleterious to cell growth (Santos-Rosa *et al*. 2005). Nem1p is a member of the haloacid dehalogenase (HAD) superfamily and harbours the

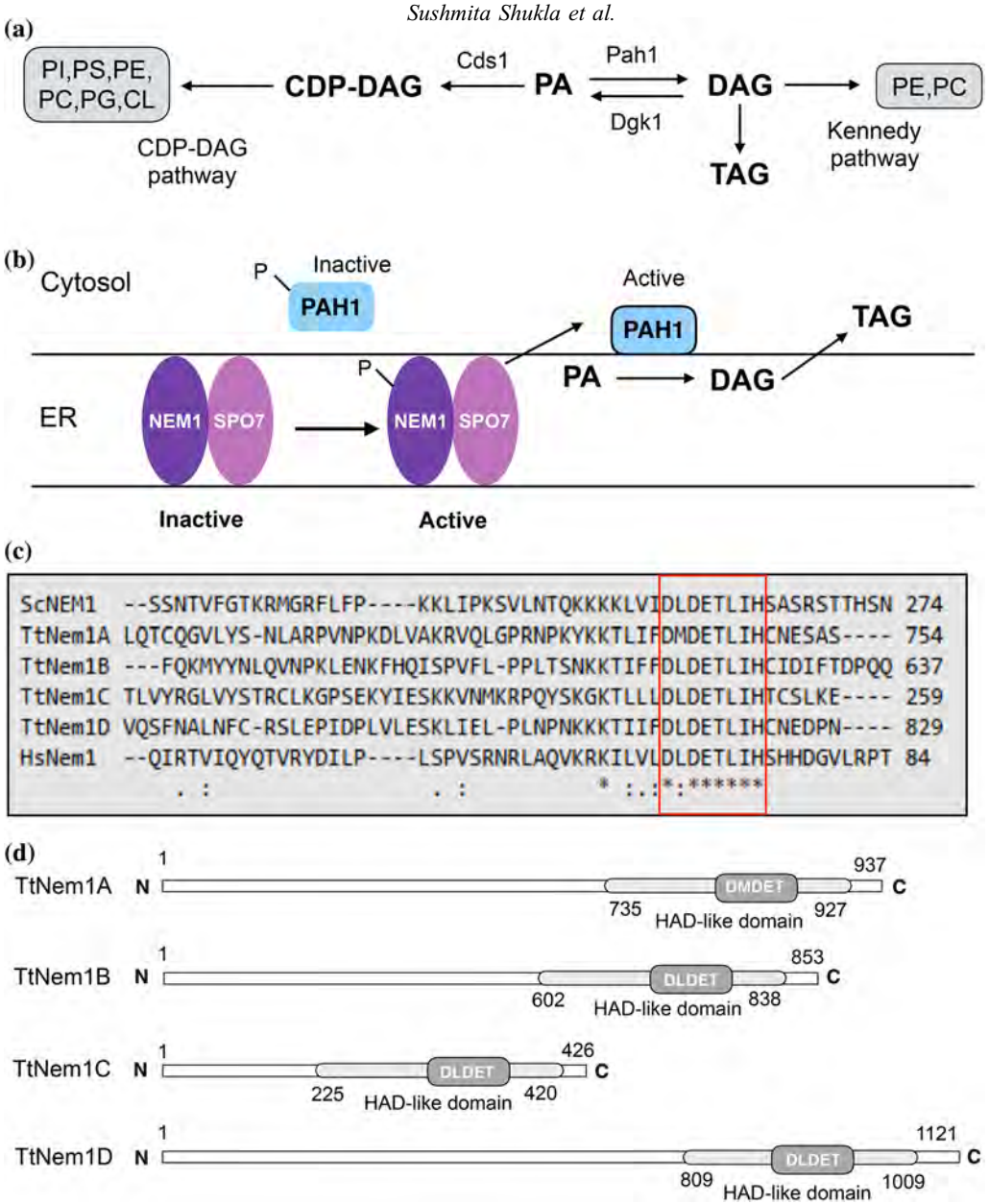

Figure 1. Function, domain organization and sequence analysis of Nem1 protein. (**a** and **b**) Schematic representation of the role of Pah and Nem1 in lipid biosynthesis. PI, phosphatidylinositol; PS, phosphatidylserine; PE, phosphatidylethanolamine; PC, phosphatidylcholine; PG, phosphatidylglycerol; CL, cardiolipin; cds1, phosphatidate cytidylyltransferase 1; pah1, phosphatidate phosphatase; dgk1, diacylglycerol kinase 1; DAG, diacylglycerol; TAG, triacylglycerol; ER, endoplasmic reticulum; NEM1, nuclear envelope morphology protein 1; SPO7, sporulation-specific protein 7. (**c**) Multiple alignments showing partial amino-acid sequences of Nem1 proteins from *S. cerevisiae*, *T. thermophila* and *H. sapiens*. (**d**) Domain organization of TtNem1A, TtNem1B, TtNem1C and TtNem1D. HAD like domain harbouring DXDXT motif is also shown.

conserved DXDXT catalytic motif (Kim *et al*. 2007). *CTDNEP1* (C-terminal domain nuclear envelope phosphatase 1, formerly known as Dullard) and *NEP1-R1* (nuclear envelope phosphatase 1-regulatory subunit 1, initially known as *TMEM188*) are the mammalian orthologues of *NEM1* and *SPO7*, respectively (Han *et al*. 2012). The human *CTDNEP1–NEP1R1* complex can functionally replace yeast *NEM1–SPO7* suggesting that Nem1–Spo7 phosphatase is evolutionarily conserved between yeast and mammals (Kim *et al*. 2007).

Tetrahymena thermophila is a unicellular protozoan ciliate, in the lineage Alveolata, and therefore much more distantly related to mammals or yeast than these are to one another (Parfrey *et al*. 2006; Adl *et al*. 2012). One well-

studied feature of *Tetrahymena* is nuclear dimorphism. Each cell contains two structurally and functionally different nuclei: a transcriptionally inert diploid germline micronucleus (MIC) and a transcriptionally active polyploid somatic macronucleus (MAC) (Mobberley *et al*. 1999; Turkewitz *et al*. 2002; Orias et al. 2011). *Tetrahymena* possesses two *PAH* homologues, *TtPAH1* (TTHERM_00189270) and *TtPAH2* (TTHERM_00215970). Earlier studies have shown that *TtPAH1* plays a role in regulating lipid homeostasis and maintaining ER/nuclear morphology and is evolutionarily conserved across eukaryotic lineages (Pillai *et al*. 2017a). In contrast, *TtPAH2* does not regulate lipid droplet biogenesis or ER/nuclear morphology but has a specific role in respiration (Pillai *et al*. 2017b).

In this study, we sought to characterize the protein phosphatase complex involved in regulation of lipid homeostasis and membrane biogenesis *via* TtPah1 in *Tetrahymena*. To that end, we considered four putative *NEM1* homologues in the *Tetrahymena* genome, called *NEM1A*, *NEM1B*, *NEM1C* and *NEM1D*. We established that *NEM1B* regulates lipid droplet biogenesis *via TtPAH1*. Our findings suggest the presence of a conserved cascade for cell-cycle regulation of lipid homeostasis and membrane biogenesis in *Tetrahymena*.

2. Materials and methods

2.1 *Tetrahymena strains and culture conditions*

Wild-type *Tetrahymena* strains, B2086 and CU428.1 were grown in SPP medium that consists of 2% proteose peptone, 0.2% glucose, 0.1% yeast extract and 0.003% ferric EDTA sodium salt at 30 °C with constant shaking at 90 rpm speed (Orias *et al*. 2000). To induce conjugation, cells of different mating types (B2086 and CU428.1) growing in the mid-log phase were washed and starved in DMC (0.17 mM sodium citrate, 0.1 mM NaH_2PO_4, 0.1 mM Na_2HPO_4, 0.65 mM $CaCl_2$ and 0.1 mM $MgCl_2$) for 16–24 h at 30 °C. An equal number of cells of the complementary mating types were mixed and incubated at 30 °C without shaking to initiate conjugation.

2.2 *Yeast strains and growth conditions*

Cells were grown either in synthetic media (SD media) consisting of 2% glucose, 0.17% yeast nitrogen base, 2.5% ammonium sulfate, along with the appropriate amino acid and nucleoside base or in YPD media at 30 °C (Sherman 2002). To evaluate growth analysis, yeast cells grown in the early logarithmic phase were serially diluted (10-fold) and 5 µL of each dilution was spotted onto the solid SD media lacking leucine and uracil, and incubated at 30 °C for 2–4 days.

2.3 *Generation of yeast expression constructs*

Because of the unusual genetic code of *Tetrahymena* (Horowitz and Gorovsky 1985), the coding regions of *TtNEM1A*, *TtNEM1B* and *TtNEM1D* were commercially synthesized by Invitrogen with codon optimization for yeast expression and the required restriction sites were added at both the ends. TtNem1 genes were cloned into the yeast expression vector YCplac111 using SalI and BamHI restriction sites.

2.4 *Yeast complementation assay*

The functional conservation of Nem1p from *Tetrahymena* to yeast was assessed using plasmid complementation study by testing the ability to rescue the aberrant nuclear phenotype of the yeast *nem1*Δ cells. All the yeast strains used in this study are derivatives of BY4741 (genotype MATa his3Δ0 leu2Δ0 met15Δ0 ura3Δ0) and were kindly provided by Ramon Serrano (-ooo). To examine the nuclear envelope morphology, the *nem1*Δ cells of yeast expressing *pUS-GFP-URA* were transformed with single copy LEU2 plasmids harbouring the *TtNEM1A*/*TtNEM1B*/*TtNEM1D* gene of *Tetrahymena* or empty vector YCplac111. Transformations in yeast were performed by the standard lithium acetate protocol (Gietz and Woods 2001). Transformants acquiring both constructs were grown in the synthetic media containing histidine, methionine and 2% glucose at 30 °C for 3 days. Images of ∼100 cells from three independent experiments were acquired by using a confocal microscope (Zeiss, LSM-780) for analysing the nuclear membrane morphology.

2.5 *Growth rate*

The wildtype, *ΔTtnem1B*, *ΔTtnem1C* and *ΔTtnem1D* cells were incubated at 30 °C with shaking at 90 rpm. When the cell number reached 1×10^5/mL, cells were counted using a haemocytometer at 2 h intervals after fixation with formalin. The averaged cell density, using biological triplicates for each cell type, was plotted against time.

2.6 *Disruption of TtNEM1 homologues*

5′UTR and 3′UTR of *TtNEM1* homologues were polymerase chain reaction (PCR) amplified and cloned into the pCRII vector (Invitrogen). To amplify 5′UTR, SacI and EcoRI restriction sites were incorporated into the forward and reverse primers, respectively (table 1). For amplification of 3′UTR, EcoRI and XhoI restriction sites were included in the forward and reverse primers, respectively (table 1). Finally, the *NEO3* cassette was introduced between 5′UTR and

Table 1. Oligonucleotides used in this study

Oligo name	Sequence
S105_Nem1B_W	CACCATGCATCACCATCACCATCACATGAAAAAAAGCAAGATACAG
S106_Nem1B_C	ATT TTA TCC TTA AAT GTT CTT TG
S107_Nem1C_W	CACCATGCATCACCATCACCATCACATGGATAAGTTATTTCAC TT
S108_Nem1C_C	TCA TAT TCC TAA CTC TTC T
S109_Nem1A_W	CACCATGCATCACCATCACCATCACATGAAGAATAATCAGAATAATTC
S110_Nem1A_C	TCA TAT TCC TAA CTC TTC T
5′UTR.Nem1A.F	GCGAGCTCGATTTATATTTTCAAAGATACAAAAGTG
5′UTR.Nem1A.R	GCGAATTCAAAACTTATTGATTGATTGTATTATCTAT
3′UTR Nem1A.F	GCGAATTCCAAATACTAAAACTAAAAAATTAAGATTATG
3′UTR Nem1A.R	GCCTCGAGCAAAATAATAAAATTAGTAAAACAAGAGG
5′ UTRNem1D.F	GCGAGCTCGAT GAT ACT GAT GAT GAA GTA ATG A
5′UTRNem1D.R	GCGAATTCTAA TAA TCT TTT TGA CAA ACT TGA TTT AC
3′UTR Nem1D.F	GCGAATTCGTA TAG ATA GAT AGA AAT ATA AAT AGA TC
3′UTR Nem1D.R	GCCTCGAGTAA TAG GAT ATT TAT GTA AAG ATT TTG
S117_Nem1D5′_W	GAGCTCGAT GAT ACT GAT GAT GAA GTA ATG A
S118_Nem1D5′_C	GAATTC TAA TAA TCT TTT TGA CAA ACT TGA TTT AC
S119_Nem1D3′_W	GAATTCGTA TAG ATA GAT AGA AAT ATA AAT AGA TC
S120_Nem1D3′_C	CTCGAGTAA TAG GAT ATT TAT GTA AAG ATT TTG
S121_5′Nem1B_F	GCGAGCTC GAC AAT GATTTTGAAGTAATATAT GTA AAT C
S122_5′Nem1B_R	GCGAATTC GTA AAA ATA ATA ATC TGC CTT GAT GAG
S123_3′Nem1B_F	GCGAATTC CTC TAA TAG CTC GAC AAA TCA ATA
S124_3′Nem1B_R	GCCTCGAG GAT AAA GTC ACT AAA TTA AGA ATT TTC A
S125_5′Nem1A_F	GCGAGCTC ACA TTA AAT CAT CAA TTC AAA AAC ATA T
S126_5′Nem1A_R	GCGAATTC T AAT GCT ACT ATT ATT GCT GTT GAA
S127_3′Nem1A_R	GCCTCGAG CAAGAGGATAAGTGGAGAAATTA
S132_Nem1A_F	AGTTAACAAAGATGACTCCAATGT
S133_Nem1A_R	CCGGTTTCTGCTTTGGTGTT
S134_Nem1B_F	AGACTTACAAAGAGACTTCTCGA
S135_Nem1B_R	GAGAAGCCATAGAAGGAGGCT
S140_Nem1A genesyn_F.P.	GC CAT ATG GAA TTC CTC GAG GTC GAC ATG AAG AAT AAT CAG AAT AAT TCA GG
S141_Nem1A genesyn_R.P.	GCGCGGCCGCAAGCTTGGGCCCGGATCCTCATAAGCTCTTTTTATAGAGATTTTC
S142_Nem1B genesyn_F.P.	GCCAT ATG GAATTC CTC GAG GTC GAC ATGAGTTCTTTCAAGAGTTCTTCT
S143_Nem1B genesyn_R.P.	GC GCGGCCGCAAGCTTGGGCCCGGATCC TCAATATTGATTTGTCGAGCTATTAG
S144_Nem1D genesyn_F.P.	GC CAT ATG GAA TTC CTC GAG GTC GAC ATG AAA ATG AAC AAA GAA TTT GGAG
S145_Nem1D genesyn_R.P.	GC GCGGCCGCAAGCTTGGGCCCGGATCC TCAATTGTTGCTATCTTTGATAAGTT
S146_smp2.1_F	GCGTTTAAACCTCGAGATGAGTGTTTTAAAAAAACTACAG
S147_smp2.1_R	GCGGGCCCTCATTCGCTTAATAGCTGGTTAAT
S148_smp2_F	CAGCAGGTAGCTCAGC
S149_smp2_R	AAA TCT TGA CTG GGT CCT G
S172_5′Nem1C_F	GCGAGCTCTTCTAAAGAATTAAATGATACAACCATT
S173_5′Nem1C_R	GCGAATTCCTGCTTAAAAGTGAAATAACTTATCC
S174_3′Nem1C_F	GCGAATTCAGAAGAGTTAGGAATATGATTAGT
S175_3′Nem1C_R	GCCTCGAGAATTGTAGTTTACTTGCTAAAGTT
S176_Nem1C.F	AGGCCATAATACTCAAAAGGAA
S177_Nem1C.R	GTGGAACTGCTTGCTGTGAA
S178_ScNem1.F	CAGGGTCACTTGGTGGAAGT
S179_ScNem1.R	AACTGGATGGGAAGGAGCTT
Alpha tubulin_F	CCTCCCCCTAAGTCTCAACC
Alpha tubulin_R	CGAAGGCAGAGTTGGTGA TT

3′UTR of the corresponding homologues using the EcoRI restriction site. The resulting knockout construct was linearized by digesting with SacI and XhoI restriction enzymes and introduced biolistically into vegetative *Tetrahymena* by particle bombardment (Bruns and Cassidy-Hanley 1999). The complete replacement of endogenous *TtNEM1* homologues was achieved by growing the transformants in the presence of increasing concentrations of paromomycin sulphate (up to 1.2 mg/mL) with 1 μg/mL cadmium chloride. The knockout strains were confirmed by reverse transcription PCR (RT-PCR) after passaging (8 passages) them in the absence of drug.

2.7 *RT-PCR analysis*

Total RNA was isolated from 3×10^5 vegetative wild-type as well as Δ*Ttnem1B* and Δ*Ttnem1D* strains using a SV Total RNA isolation kit (Promega) following the manufacturer's guidelines. For standard RT-PCR, cDNA synthesis was carried out from 2 μg of total RNA with SuperScriptII reverse transcriptase and random hexamer primers (Invitrogen). PCRs were performed with 100 ng cDNA using *TtNEM1*-specific primers and alpha-tubulin (*ATU1*) primers (table 1) in the same reaction for 28 or 35 cycles using Taq polymerase.

2.8 *Staining and microscopy*

For staining lipid droplets, *Tetrahymena* cells were pelleted by centrifugation (1100*g* for 2 min) at room temperature, washed with DMC and fixed with 4% paraformaldehyde. Fixed cells were washed with 10 mM HEPES and resuspended in freshly prepared Oil Red O solution. Cells were tapped briefly and incubated in the dark in a rotating mixer at room temperature for 10 min. Stained cells were washed thrice with 10 mM HEPES and were resuspended in 10 mM HEPES before imaging using a confocal microscope. For quantitation of the number and area of lipid droplets we have stacked the 3D image and used the droplet finder plugin of ImageJ software. We have also counted the lipid droplet number manually to confirm the results obtained using ImageJ software.

For endoplasmic reticulum (ER) staining, the *Tetrahymena* cells were grown to a density of $3–4\times10^5$ and 0.5 μM ER-Tracker Green dye (Invitrogen) was added to the culture and incubated for 60 min before fixing the cells with 4% paraformaldehyde (50 mM HEPES, pH 7.5).

For Oil Red O staining, images were taken at 543 nm excitation/619 nm emission and for ER-Tracker Green images were taken at excitation/emission – 504/511 nm. 3–5 μL of cells were mounted on glass slides, covered with cover glasses and sealed with nail polish and imaged with a Zeiss LSM780 confocal microscope. The step size of the consecutive *z*-slices was 0.5 μm.

To quantitate ER content, the stacked images of ER-tracker Green-stained cells were analysed by image after sum intensity projection. The mean intensity values were plotted for both wild-type ($n = 70$) and Δ*Ttnem1C* ($n = 60$) cells using box plot.

2.9 *Sequence analysis*

Amino acid sequences of Nem1 homologues were obtained from the TGD database (*http://ciliate.org/index.php/home/welcome*). Protein sequence analysis and identification of phosphatase domain (characteristic of Nem1) were performed using the Interpro program (*https://www.ebi.ac.uk/interpro/*).

2.10 *Lipid analysis*

The total lipids were extracted from *Tetrahymena* cells by the method of Bligh and Dyer (1959). Lipids were extracted in chloroform and the isolated lipids were then dried under N_2 and dissolved in 50 μL of chloroform. Total lipids were quantitated using the phospho-vanillin method (Knight *et al*. 1972; Johnson *et al*. 1977). For this purpose, the dried lipid samples were mixed with 100 μL of sulphuric acid and heated for 10 min followed by addition of 2.4 mL vanillin reagent (600 mg of vanillin, 100 mL of water, 400 mL of 85% phosphoric acid). Pink colour was allowed to develop for 5 min and absorbance was recorded at 490 nm using a spectrophotometer.

For quantitation of TAG levels, the samples were separated by thin-layer chromatography on 20-cm silica gel glass plates (Merck) using 80:20:2 hexane/diethyl ether/acetic acid (vol/vol/vol) as a mobile phase. The plate was treated with 3% of copper(II) acetate in 8% (v/v) phosphoric acid and charred to develop lipid spots by incubating at 180°C.

3. Results

3.1 *Domain structure and sequence analysis of the NEM1 homologues*

Three genes TTHERM_00262970 (*NEM1A*), TTHERM_00685940 (*NEM1C*) and TTHERM_00688650 (*NEM1D*) are designated as putative *NEM1* homologues in the *Tetrahymena* genome database. Another gene TTHERM_00473100 (*NEM1B*) was also included in this study since previously it was designated as putative *NEM1* homologue in the same database. Amino acid sequence analysis of Nem1 homologues in *Tetrahymena* showed that all four harbour a conserved DXDXT catalytic phosphatase motif in the C-terminal domain (figure 1c), but they differ significantly in their overall sizes. Nem1A codes for a protein of 937 amino acids; Nem1B codes for a protein of 926 amino acids; Nem1C consists of 426 amino acids and Nem1D consists of 1121 amino acids (figure 1d). In comparison, *S. cerevisiae* Nem1p consists of 446 amino acids while human *NEM1* consists of 244 amino acids. Thus, the *Tetrahymena NEM1* homologues except TtNem1C are larger than the yeast and mammalian proteins. The amino acid sequence identity of TtNem1A, TtNem1B, TtNem1C and TtNem1D with *S. cerevisiae* Nem1p was 24.16%, 22.75%, 24.22% and 23.88%, respectively.

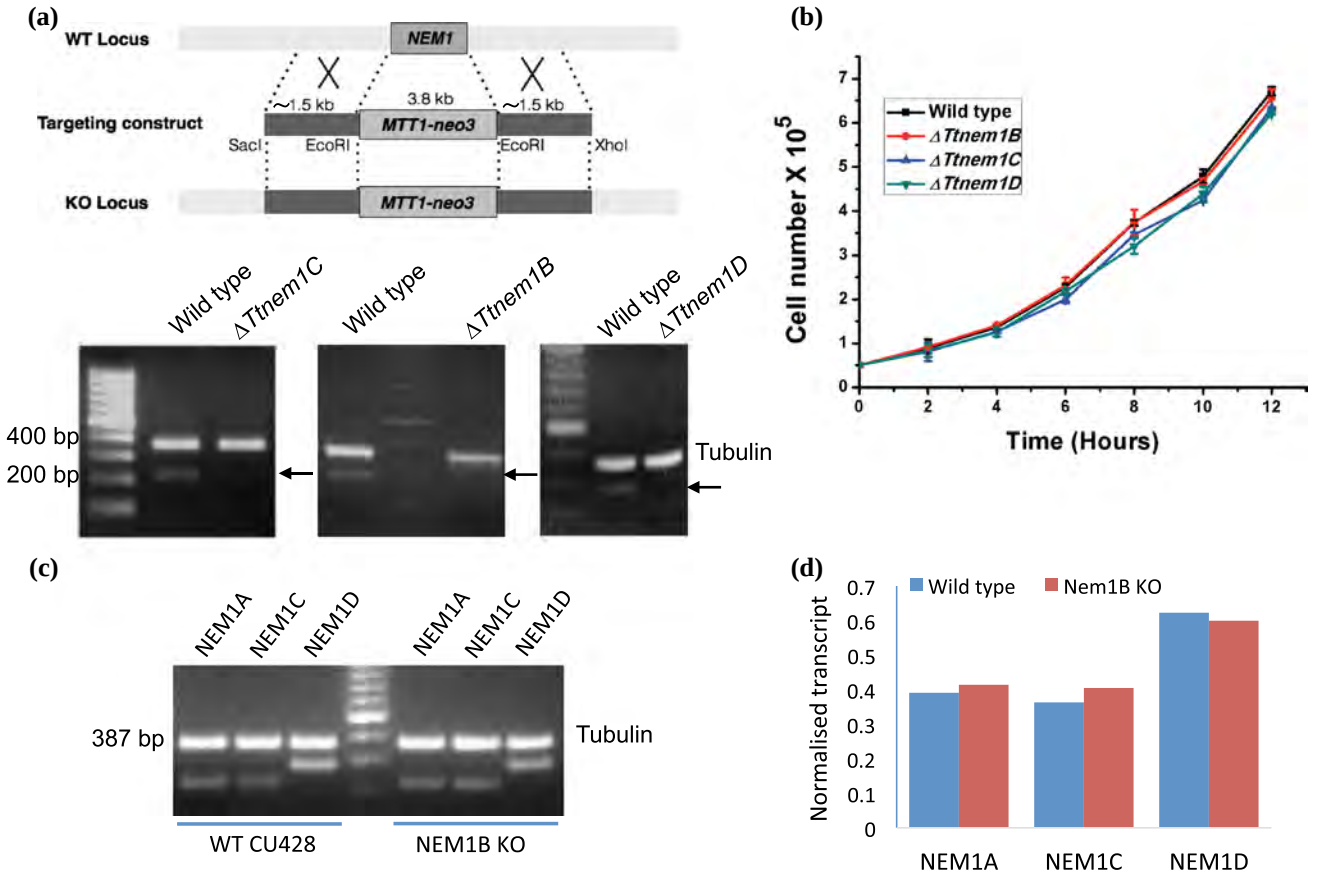

Figure 2. *TtNEM1B*, *TtNEM1C* and *TtNEM1D* are dispensable for normal growth of vegetative *Tetrahymena* cells. (**a**) The top panel shows schematic of the gene deletion strategy to generate knockout construct used to disrupt individual TtNEM1 homologues in the MAC. The bottom panel shows RT-PCR analysis of Δ*Ttnem1C* cells (left), Δ*Ttnem1B* cells (middle) and Δ*Ttnem1D* cells (right) along with wild-type cells. The top band corresponds to alpha-tubulin (387 bp). The absence of band of the respective gene (indicated by an arrow) in Δ*Ttnem1C*, Δ*Ttnem1B* and Δ*Ttnem1D* cells but their presence in the wild-type cells confirms that knockout is complete. (**b**) Growth curve of *Tetrahymena* wild-type, *ΔTtnem1B*, *ΔTtnem1C* and *ΔTtnem1D* cells. (**c**) Semi-quantitative RT-PCR showing expression of *TtNEM1A*, *TtNEM1C* and *TtNEM1D* in wild-type (WT CU428) and Δ*Ttnem1B* cells (NEM1B KO). Lane 4, standard molecular weight marker; lanes 1–3, amplified products of cDNA from wild-type cells; lanes 5–7, amplified products of cDNA from Δ*Ttnem1B* cells. The top band in lanes 1–3 and 5–7 corresponds to alpha-tubulin (387 bp). The bottom band in lanes 1 and 5 corresponds to TtNEM1A (221 bp), in lanes 2 and 6 corresponds to TtNEM1C (220 bp), in lanes 3 and 7 corresponds to TtNEM1D (282 bp). (**d**) The graph shows quantitation of *TtNEM1A*, *TtNEM1C* and *TtNEM1D* after normalization with the alpha-tubulin. The number of experimental replicates was three. The expression of *TtNEM1A*, *TtNEM1C* and *TtNEM1D* is not enhanced by the loss of *TtNEM1B*.

3.2 *Nem1B, Nem1C and Nem1D are dispensable for normal growth of Tetrahymena*

To assess which of the four *Tetrahymena NEM1* genes might regulate lipid homeostasis and membrane biogenesis, we targeted the disruption in the somatic MAC of each of these genes. Gene disruption was performed by replacing the endogenous macronuclear open-reading frames with the *NEO3* cassette through homologous recombination (figure 2a). Replacement of all the macronuclear copies of *NEM1B*, *NEM1C* and *NEM1D* by the drug-resistance cassette was confirmed by RT-PCR, indicating that these genes are not essential for *Tetrahymena* growth (figure 2a). The knockout lines are indicated as Δ*Ttnem1B*, Δ*Ttnem1C* and Δ*Ttnem1D*. In contrast, we were unable to obtain a knockout of *NEM1A* despite repeated attempts. The failure in generating the *NEM1A* knockout strain was not due to the lack of recombination in this locus since we were able to obtain initial transformants, suggesting that one or few copies of *NEM1A* were replaced with the drug-resistance cassette. This result indicates that *NEM1A* is essential for *Tetrahymena* viability under these conditions.

We measured the growth rates of the *ΔTtnem1B*, *ΔTtnem1C* and *ΔTtnem1D* mutant cells and compared with the wild-type cells. The growth of all the mutants was similar to that of the wild-type cells (figure 2b), suggesting that these homologues are not required for the laboratory growth of *Tetrahymena*. To

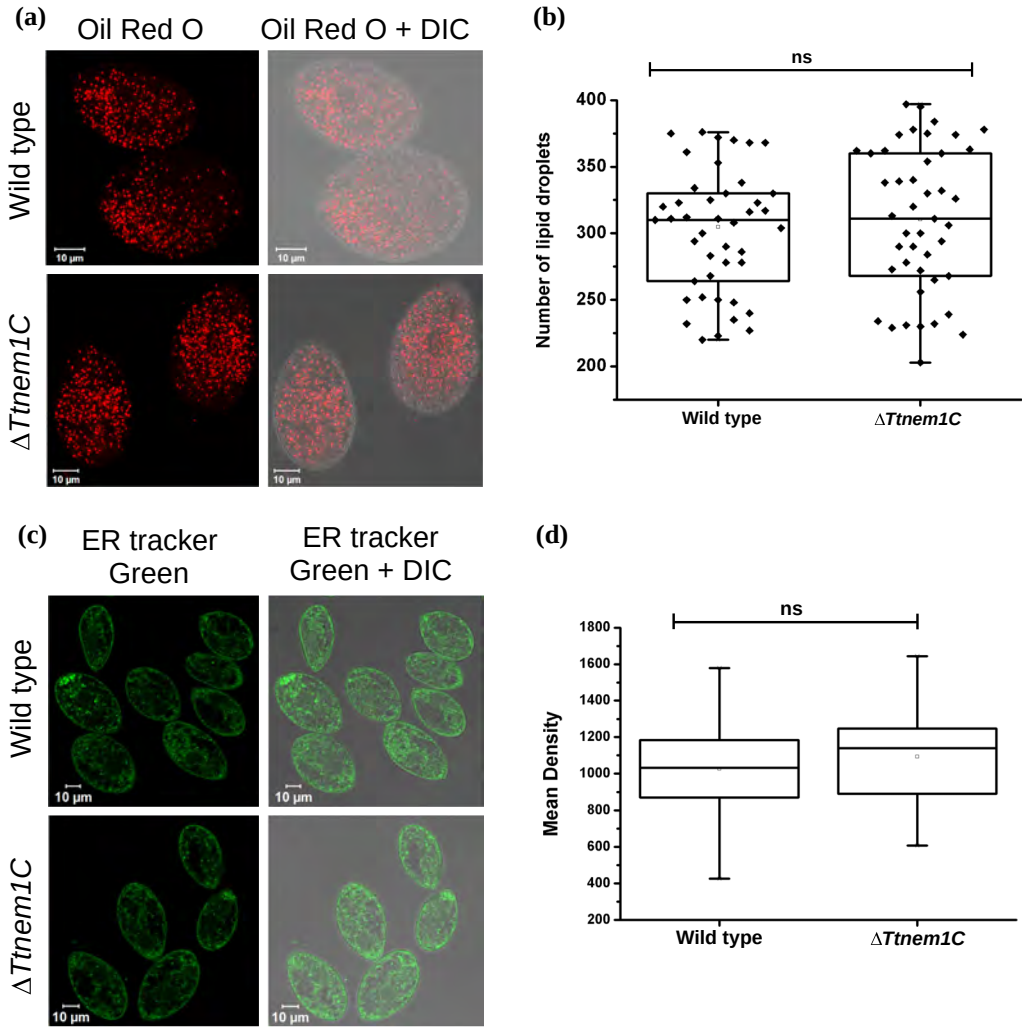

Figure 3. TtNem1C does not regulate lipid droplet number and ER morphology in *Tetrahymena*. (**a**) Confocal images of wild-type and, *ΔTtnem1C Tetrahymena* cells showing lipid droplets after staining with Oil Red O dye. (**b**) Box plot showing the distribution of lipid droplet numbers in wild-type and *ΔTtnem1C Tetrahymena* cells. No significant difference (indicated as 'ns') in the number of lipid droplets between *ΔTtnem1C* and wild-type cells was observed as analysed by the Kruskal–Wallis test ($p<0.01$). (**c**) Confocal images of wild-type and *ΔTtnem1C Tetrahymena* cells stained with ER-Tracker Green showing ER morphology. (**d**) Box plot showing the mean ER content in wild-type and *ΔTtnem1C* cells as measured by sum intensity projection of the stacked images. There was no significant difference in the mean ER content between *ΔTtnem1C* and wild-type cells as analysed by the Kruskal–Wallis test ($p<0.01$). ns represents not significant.

evaluate if the lack of growth defect is due to compensatory overexpression of the remaining homologues, we carried out semi-quantitative RT-PCR. The results show that the lack of growth defect in *ΔTtnem1B* cells is not due to the overexpression of the other homologues (figure 2c and d).

3.3 *Nem1C in Tetrahymena, though of similar size to yeast Nem1, is not functionally equivalent*

Nem1p dephosphorylates Pah1p and regulates lipid homeostasis and membrane biogenesis. Of the *T. thermophila* homologues, the percentage sequence identity of TtNem1C with ScNem1 is 24.22, which is similar to those of the other three *Tetrahymena NEM1* homologues. TtNem1C is most similar in size to ScNem1 and is therefore the putative *bona fide* orthologue. To evaluate the role of Nem1C in lipid droplet biogenesis, lipid droplets of both wild-type and Δ*Ttnem1C Tetrahymena* strains were stained using a neutral lipid dye Oil Red O. Confocal image analysis showed no significant reduction in lipid droplet number in Δ*Ttnem1C* compared with the wild-type cells (figure 3a and b). The average lipid droplet number per cell was 304 in wild-type cells ($n = 50$) and 310 in Δ*Ttnem1C* ($n = 50$). To find out if *NEM1C* regulates ER morphology, we stained both wild-type and Δ*Ttnem1C* cells with the ER-Tracker dye and

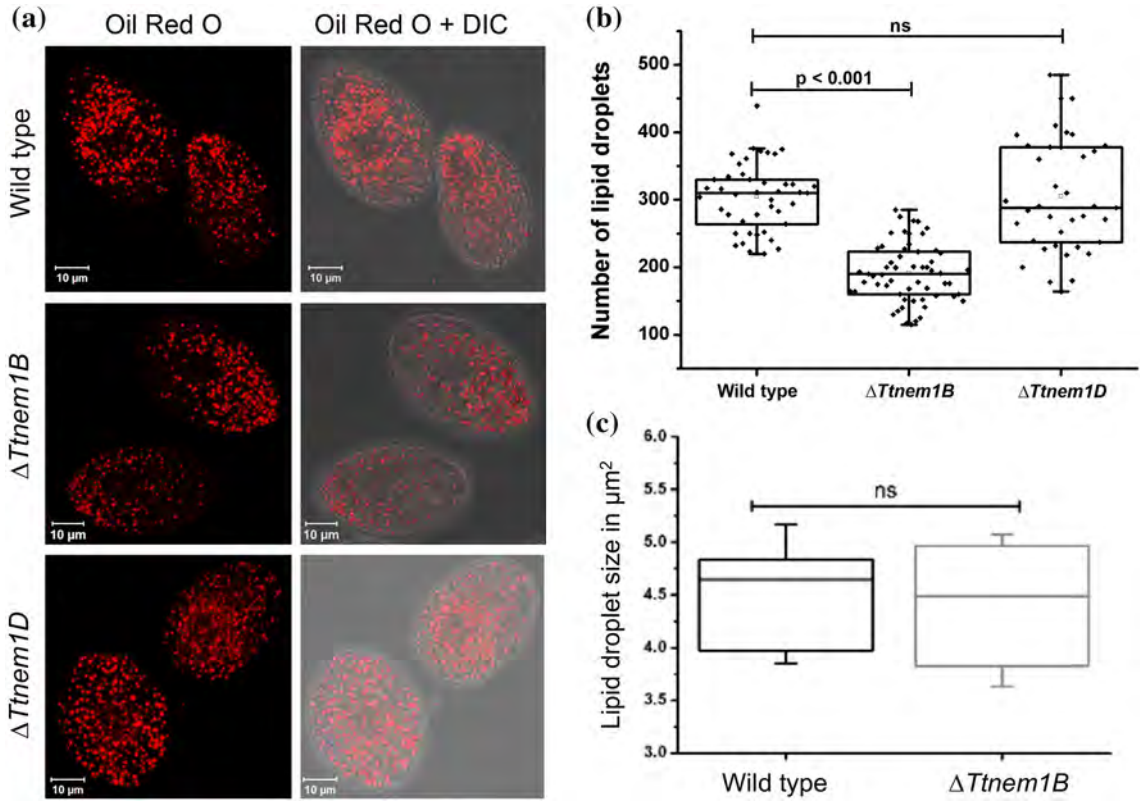

Figure 4. TtNem1B maintains lipid droplet number in *Tetrahymena*. (**a**) Confocal images of wild-type, *ΔTtnem1B* and *ΔTtnem1D Tetrahymena* cells showing lipid droplets after staining with Oil Red O dye. (**b**) Box plot showing the distribution of lipid droplet numbers in wild-type, *ΔTtnem1B* and *ΔTtnem1D Tetrahymena* cells. A significant difference was observed in the number of lipid droplets between *ΔTtnem1B* and wild-type cells ($p<0.001$) whereas no significant difference was observed in the number of lipid droplets between *ΔTtnem1D* and wild-type cells as analysed by the Kruskal–Wallis test ($p<0.01$). (**c**) Box plot showing the size distribution of lipid droplet in wild type ($n = 20$) and *ΔTtnem1B* ($n = 20$) *Tetrahymena* cells. No significant difference was observed in the size of lipid droplets as analysed by the Kruskal–Wallis test ($p<0.01$).

evaluated ER morphology by analysing confocal images. We did not find any visible defect in ER morphology and ER content of Δ*Ttnem1C* cells compared with the wild-type cells (figure 3c and d). These results led us to conclude that though TtNem1C is similar in size, it is not functionally equivalent to yeast Nem1.

3.4 *Loss of Nem1B regulates lipid droplet biogenesis in Tetrahymena*

Since *NEM1C* did not regulate lipid droplet biogenesis and ER morphology in *Tetrahymena*, we investigated the potential role of other *NEM1* homologues in this process. Lipid droplets of wild type, as well as both Δ*Ttnem1B* and Δ*Ttnem1D* were stained with Oil Red O and visualized by confocal imaging (figure 4a). As shown in figure 4b, the average lipid droplet number per cell was 304 in wild-type cells ($n = 44$), 202 in Δ*Ttnem1B* ($n = 59$) and 305 in Δ*Ttnem1D* ($n = 38$). The loss of Nem1B reduced lipid droplet numbers significantly (33%) whereas no reduction in lipid droplet number was observed in Δ*Ttnem1D*. The size of the lipid droplets was not affected significantly upon deletion of *TtNEM1B* (figure 4c), suggesting that the reduced number of lipid droplets in Δ*Ttnem1B* is not due to the increased lipid droplet size. These results suggest that Nem1B regulates lipid droplet biogenesis in *Tetrahymena*.

3.5 *Overexpression of TtPAH1 partially restores lipid droplet biogenesis in Δnem1B mutant Tetrahymena cells*

In *S. cerevisiae*, Nem1 functions *via* Pah1 and overexpression of *PAH1* rescues defects due to loss of *NEM1* function. In *Tetrahymena*, we previously showed that loss of *TtPAH1* causes a severe reduction in lipid droplet number and overexpression of *TtPAH1* leads to increased lipid droplet number (Pillai *et al*. 2017a). To assess if Nem1B regulates lipid droplet biogenesis *via* Pah1 in *Tetrahymena*, we

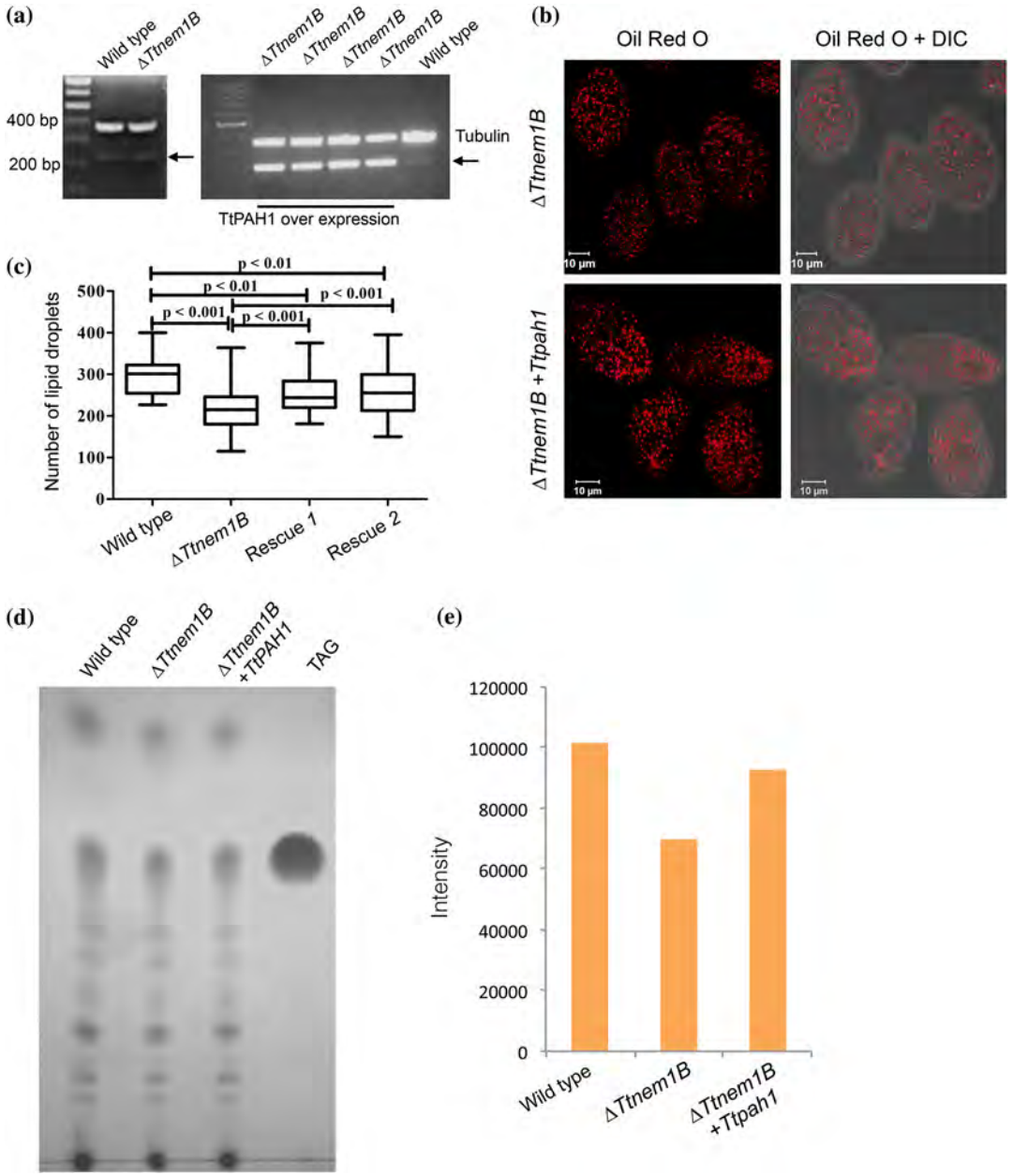

Figure 5. Overexpression of *TtPAH1* partially restores lipid droplet number in Δ*Ttnem1B Tetrahymena* cells. (**a**) RT-PCR analysis of *TtPAH1*. The left panel shows amplified products of cDNA from wild-type cells (lane 2) and *ΔTtnem1B* cells (lane 3); lane 1 is the standard molecular weight marker. In lanes 2 and 3, the top band corresponds to alpha-tubulin (387 bp) and the bottom band corresponds to *TtPAH1* (220 bp). The right panel shows amplified products of cDNA from *ΔTtnem1B* cells transformed with *TtPAH1* (lanes 2–5), from wild-type *Tetrahymena* cells (lane 6); lane 1 is the standard molecular weight marker. In lanes 2–6, the top band corresponds to alpha-tubulin (387 bp) and the bottom band corresponds to *TtPAH1* (220 bp). No visible difference in expression of *TtPAH1* was observed upon deletion of *TtNem1B* (left panel). As expected, significant overexpression of *TtPAH1* was observed in *ΔTtnem1B* cells transformed with *TtPAH1* (right panel). (**b**) Confocal images of *ΔTtnem1B* and *ΔTtnem1B* cells over-expressing *TtPAH1* showing lipid droplets after staining with Oil Red O dye. (**c**) Box plot showing lipid droplet numbers in wild-type cells, *ΔTtnem1B* cells and cells overexpressing *TtPAH1* in *ΔTtnem1B* cells. Rescue 1 and rescue 2 are independent transformants overexpressing *TtPAH1* in *ΔTtnem1B* cells. An increase in lipid droplet number was observed upon overexpression of *TtPAH1* in *ΔTtnem1B* cells. The *p* values are indicated in the figure. (**d**) The total lipids extracted from wild-type, *ΔTtnem1B* and *ΔTtnem1B* cells transformed with *TtPAH1* were subjected to thin-layer chromatography to separate the neutral lipids. Samples from at least three independent cultures of each strain were analysed. We have used TAG standard to identify the appropriate position of TAG in the experimental samples. (**e**) The intensity of the bands corresponding to TAG of all three samples in the TLC plate (as shown in **d**) was measured using quantity-one software (Bio-Rad). The intensity was normalized by dividing it with the respective total lipid before plotting the graph.

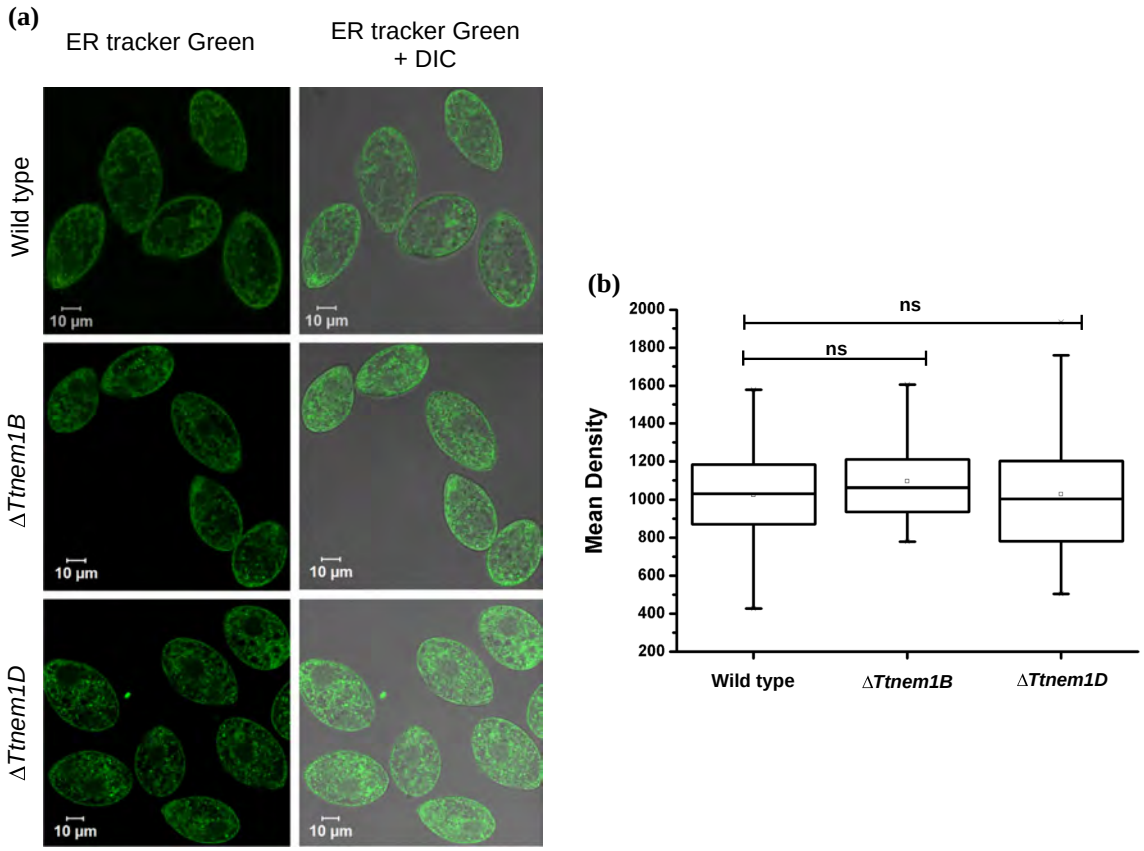

Figure 6. *TtNEM1B* and *TtNEM1D* do not regulate ER morphology. (**a**) Confocal images of wild type, *ΔTtnem1B* and *ΔTtnem1D* cells stained with ER-Tracker Green showing ER morphology. (**b**) Box plot showing the mean density of ER-Tracker dye in wild type, *ΔTtnem1B* and *ΔTtnem1D* cells as measured by sum intensity projection of the stacked images. The *p* values are indicated in the figure.

overexpressed *TtPAH1* in Δ*Ttnem1B* cells, evaluated the lipid droplet numbers in these cells and compared with Δ*Ttnem1B* cells. The overexpression of *TtPAH1* in Δ*Ttnem1B* cells was confirmed by RT-PCR analysis (figure 5a). Analysis of confocal images after Oil Red O staining showed that the mean lipid droplet number was 257 per cell in Δ*Ttnem1B* cells overexpressing *TtPAH1* ($n = 65$), 202 per cell in Δ*Ttnem1B* cells ($n = 54$) and 304 per cell in the wild-type cells ($n = 50$) (figure 5b and c). Therefore, there was ∼50% rescue of the defect in lipid droplet number in Δ*Ttnem1B* by *TtPAH1* overexpression. These results are consistent with the idea that TtNem1B regulates lipid droplet biogenesis *via* TtPah1. We also quantitated the TAG levels in wild type, Δ*Ttnem1B* and Δ*Ttnem1B* cells overexpressing *TtPAH1* by thin-layer chromatography. As expected, the TAG level was reduced in Δ*Ttnem1B* cells compared with the wild-type cells and was increased upon over-expression of *TtPAH1* (figure 5d and e). These results suggest that *TtNEM1B* regulates lipid droplet biogenesis *via TtPAH1* by regulating the levels of TAG.

3.6 *Nem1B or Nem1D does not regulate ER structure in Tetrahymena*

In organisms including yeast and mammals, Nem1 regulates ER morphology. To investigate if Nem1B also regulates ER morphology in *Tetrahymena*, we stained both the wild-type and Δ*Ttnem1B* cells with ER-Tracker dye and evaluated ER morphology. Surprisingly, both ER morphology and ER content of Δ*Ttnem1B* cells were similar to those of the wild-type cells (figure 6a and b). Therefore, while Nem1B in *Tetrahymena* regulates lipid droplet biogenesis, it does not regulate ER morphology. Since Nem1B did not regulate ER morphology, we, therefore, assessed whether a different homologue, TtNem1D, might play that role by staining the Δ*Ttnem1D* cells with ER tracker dye. As shown in figure 6a, no visible defect was observed in ER morphology of Δ*Ttnem1D* cells, and its ER content was comparable with the wild-type cells (figure 6b). Overall, these findings establish that neither Nem1B nor Nem1D is required to regulate ER structure in *Tetrahymena*.

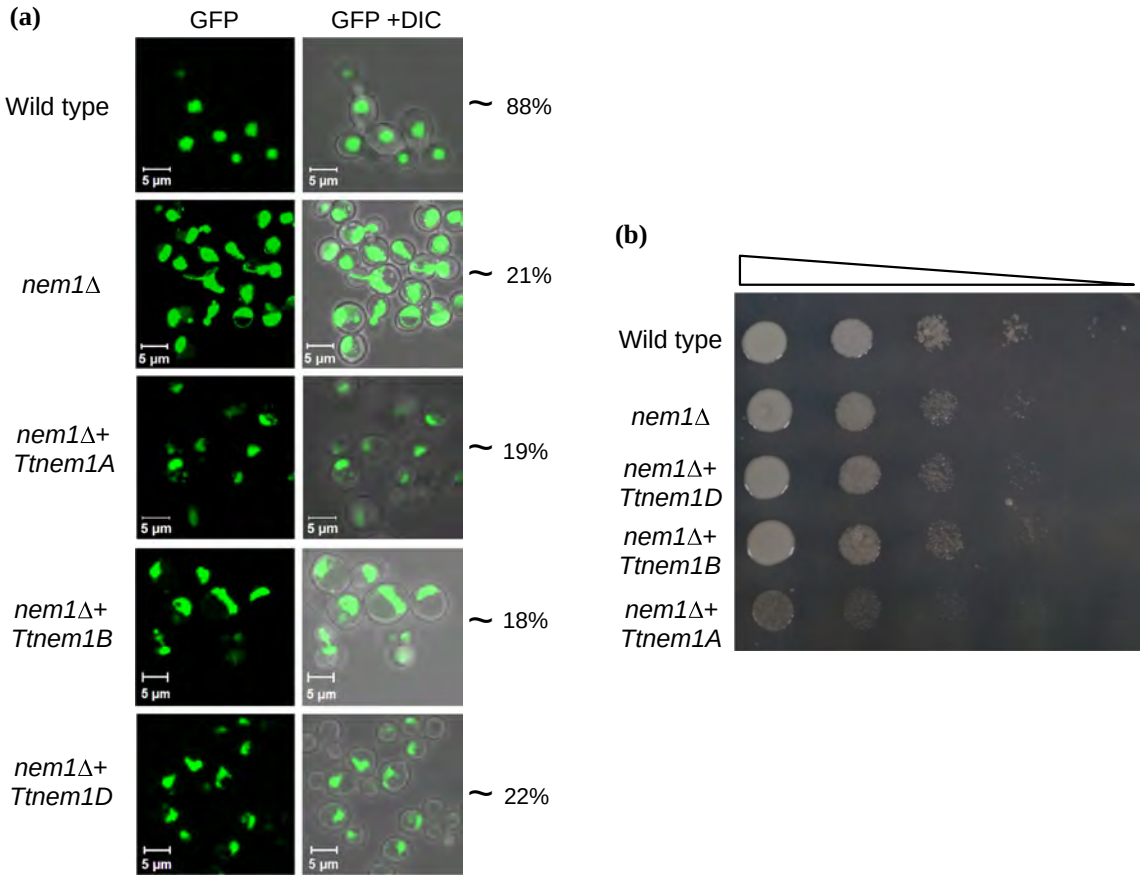

Figure 7. *TtNEM1A*, *TtNEM1B* and *TtNEM1D* homologues do not functionally replace yeast *NEM1*. (**a**) Confocal images of *nem1Δ* yeast cells transformed with either empty vector or *TtNEM1A* or *TtNEM1B*, or *TtNEM1D* along with the wild-type cells. PUS1-GFP (a nucleoplasmic marker) was expressed to visualize nuclei. *TtNEM1* homologues do not restore the aberrant nuclear morphology of the *nem1Δ* yeast cells. Three different transformants per strain were analysed and the number of cells counted for each transformant was 100 ($n = 300$). The percentage of cells containing round nucleus is indicated on the right. (**b**) The growth of *nem1Δ* yeast cells transformed with either empty vector or *TtNEM1B*, or *TtNEM1D*, or *TtNEM1A* along with wild-type yeast cells grown at 30 °C on SD media lacking leucine and uracil.

3.7 *Tetrahymena Nem1B does not functionally replace yeast Nem1*

Yeast mutants lacking *PAH1* or *NEM1* exhibit slow growth and an aberrant nuclear membrane morphology. In the mutants, the nucleus is elongated rather than spherical as in wild type, and also has projections (Siniossoglou *et al*. 1998; Santos-Rosa *et al*. 2005). Yeast Nem1 can be functionally replaced with its mammalian orthologue, CTDNEP1. Similarly, we previously found that *Tetrahymena TtPAH1* functionally complements yeast *PAH1* (Pillai *et al*. 2017a).

To investigate if *TtNEM1B* complements the deletion of yeast *NEM1*, we overexpressed *TtNEM1B* in the *nem1*Δ yeast cells and evaluated its ability to rescue the slow growth and aberrant nuclear phenotypes. A nucleoplasmic marker PUS-GFP was expressed to evaluate nuclear morphology in yeast. Surprisingly, *TtNEM1B* failed to rescue either the slow growth or aberrant nuclear morphology of *S. cerevisiae nem1*Δ (figure 7).

To examine if other *NEM1* homologues of *Tetrahymena* could replace yeast *NEM1*, we overexpressed *TtNEM1A* and *TtNEM1D* in *nem1*Δ yeast cells and monitored the nuclear morphology and growth phenotype. Neither *TtNEM1A* nor *TtNEM1D* rescued the defects (figure 7). Interestingly, we found that the growth of *nem1Δ* yeast cells overexpressing *TtNEM1A* is slower than that of *nem1Δ* yeast cells. How *TtNEM1A* affects the growth of *nem1*Δ yeast cells is not known. It is possible that TtNem1A has an inhibitory effect on some essential processes of yeast.

To exclude the possibility that the absence of rescue is due to the lack of expression, the transcripts corresponding to *TtNEM1A*, *TtNEM1B* and *TtNEM1D* were confirmed by RT-PCR analysis (data not shown).

4. Discussion

Lipid homeostasis and membrane biogenesis are regulated by a cascade comprising Pah1 (a phosphatidate phosphatase) and Nem1/Spo7 (a cell cycle-regulated protein phosphatase) complex in yeast and a similar cascade is also present in other organisms including plants, mammals, worms and flies (Golden *et al*. 2009; Nakamura *et al*. 2009; Ugrankar *et al*. 2011; Pascual and Carman 2013). Deletion of *NEM1* results in growth defect, ER/nuclear membrane defect and reduced lipid droplet number in yeast and metazoans (Gorjánácz and Mattaj 2009; Adeyo *et al*. 2011; Pascual and Carman 2013; Fernández-Murray and McMaster 2016). In this study, we investigated four putative homologues of *NEM1* in *Tetrahymena* and established that TtNem1B together with TtPah1 is involved in regulating lipid droplet biogenesis.

Previous reports have shown that the deletion of *NEM1* in yeast leads to a growth defect (Kim *et al*. 2007; Siniossoglou 2009). We found that Nem1B, Nem1C and Nem1D are not essential for cell viability.

We also found that TtNem1B regulates lipid droplet biogenesis, while neither TtNem1C nor TtNem1D appears to be required for this function. Although not definitive, these results suggest that *Tetrahymena NEM1B* may be the orthologue of *S. cerevisiae NEM1*. It is also possible that *Tetrahymena* Nem1A is involved in lipid droplet biogenesis. As mentioned earlier, we failed to generate knockout strains of *TtNEM1A* in multiple attempts suggesting that *TtNEM1A* is an essential gene. It should be noted that the cascade of lipid homeostasis and membrane biogenesis (comprising Pah1 and Nem1/Spo7 in yeast) is not essential in any organism studied so far including *Tetrahymena*. Therefore, the essentiality of *NEM1A* suggests that this *Tetrahymena* gene is involved in other as yet unknown processes.

Nem1 dephosphorylates Pah1 and regulates lipid homeostasis and membrane biogenesis (Santos-Rosa *et al*. 2005; Siniossoglou 2009; Adeyo *et al*. 2011). Overexpression of *TtPAH1* in *ΔTtnem1B* cells partially rescued the defect in lipid droplet biogenesis. The incomplete rescue may be due to limiting kinase activity needed to phosphorylate the large pool of overexpressed Pah1. These results indicate that TtPah1 together with TtNem1B forms a cascade for regulation of lipid homeostasis and membrane biogenesis in *Tetrahymena*.

Nem1 regulates lipid homeostasis and membrane biogenesis *via* Pah1 and loss of Nem1 or Pah1 function results in a defect in ER morphology (Bahmanyar *et al*. 2014; Bahmanyar 2015). Interestingly, TtNem1B was not required to maintain normal ER morphology in *Tetrahymena*. This was surprising given that TtNem1B, like Nem1 in other organisms, functions *via* Pah1 and loss of *TtPAH1* produces a clear defect in ER morphology (Pillai *et al*. 2017a). Pah1 dephosphorylates PA in the ER membrane to generate DAG which serves as the precursor for both the synthesis of TAG and the synthesis of membrane phospholipids such as PC and PE (Carman and Han 2009b; Han *et al*. 2007; Gibellini and Smith 2010; Kohlwein 2010). In addition to dephosphorylation of PA, an independent role of Pah1 as a transcriptional regulator is known in yeast and mammals (Phan *et al*. 2004; Santos-Rosa *et al*. 2005; Michot *et al*. 2010). Therefore, it is possible that Pah1 in *Tetrahymena* also has an additional, Nem1-independent function in regulating ER morphology. Alternatively, it is possible that in *ΔTtnem1B* cells the heterogeneous phosphorylation state of TtPah1 results in a cohort of protein that is sufficient to regulate ER morphology but insufficient to stimulate wild-type lipid droplet formation. Further studies are required to understand the lack of Nem1 function in regulating ER morphology.

Our earlier study showed that *T. thermophila PAH1* can functionally replace yeast *PAH1* (Pillai *et al*. 2017a). However, neither *NEM1A*, *NEM1B* nor *NEM1D* complemented the loss of yeast *NEM1*. One possible explanation is that Spo7, which directly regulates Nem1 in *S. cerevisiae*, does not recognize *Tetrahymena* Nem1 and hence fails to dephosphorylate yeast Pah1. Consistent with this idea, we could not find any *SPO7* homologue in the *Tetrahymena* genome, suggesting that the regulatory subunit of TtNem1 may have diverged drastically from Spo7.

In summary, *Tetrahymena* possesses multiple *Nem1* homologues. Of these, *TtNEM1B* is shown to be most functionally related to *NEM1* in other organisms. Our results indicate that a conserved cascade comprising Nem1 and Pah1 functions in *Tetrahymena* to regulate lipid homeostasis and membrane biogenesis.

Acknowledgements

We thank Professor Aaron Turkewitz from the University of Chicago for critical evaluation and useful comments on the manuscript. We are grateful to Ramon Serrano (Polytechnic University of Valencia, Spain) for providing us *nem1*Δ yeast strain. We also thank Symeon Siniossoglou (University of Cambridge) for providing us PUS-GFP plasmid. AN was supported by the Council of Scientific and Industrial Research (CSIR) fellowship. Grant support from DBT (BT/PR14643/BRB/10/862/2010) is gratefully acknowledged.

References

Adeyo O, Horn PJ, Lee S, Binns DD, Chandrahas A, Chapman KD and Goodman JM 2011 The yeast lipin orthologue Pah1p is important for biogenesis of lipid droplets. *J. Cell Biol.* **192** 1043–1055

Adl SM *et al.* 2012 The revised classification of eukaryotes. *J. Eukaryote Microbiol.* **59** 429–493

Bahmanyar S 2015 Spatial regulation of phospholipid synthesis within the nuclear envelope domain of the endoplasmic reticulum. *Nucleus* **6** 102–106

Bahmanyar S, Biggs R, Schuh AL, Desai A, Müller-Reichert T, Audhya A, Dixon JE and Oegema K 2014 Spatial control of phospholipid flux restricts endoplasmic reticulum sheet formation to allow nuclear envelope breakdown. *Genes Dev.* **28** 121–126

Bligh EG and Dyer WJ 1959 A rapid method of total lipid extraction and purification. *Can. J. Biochem. Physiol.* **37** 911–917

Bruns PJ and Cassidy-Hanley D 1999 Biolistic transformation of macro- and micronuclei. *Method. Cell Biol.* **62** 501–512

Carman GM and Han G 2009a Phosphatidic acid phosphatase, a key enzyme in the regulation of lipid synthesis. *J. Biol. Chem.* **284** 2593–2597.

Carman GM and Han GS 2009b Regulation of phospholipid synthesis in yeast. *J. Lipid Res.* **50**(Supplement) S69–S73.

Choi HS, Su WM, Han GS, Plote D, Xu Z and Carman GM 2012 Pho85p-Pho80p phosphorylation of yeast pah1p phosphatidate phosphatase regulates its activity, location, abundance, and function in lipid metabolism. *J. Biol. Chem.* **287** 11290–11301

Fernández-Murray JP and McMaster CR 2016 Lipid synthesis and membrane contact sites: a crossroads for cellular physiology. *J. Lipid Res.* **57** 1789–1805

Gibellini F and Smith TK 2010 The Kennedy pathway – de novo synthesis of phosphatidylethanolamine and phosphatidylcholine. *IUBMB Life* **62** 414–428

Gietz RD and Woods RA 2001 Genetic transformation of yeast. *Biotechniques* **30** 816–831

Golden A, Liu J and Cohen-Fix O 2009 Inactivation of the *C. elegans* lipin homolog leads to ER disorganization and to defects in the breakdown and reassembly of the nuclear envelope. *J. Cell Sci.* **122** 1970–1978

Gorjánácz M and Mattaj IW 2009 Lipin is required for efficient breakdown of the nuclear envelope in *Caenorhabditis elegans*. *J. Cell Sci.* **122** 1963–1969

Han GS and Carman GM 2010 Characterization of the human LPIN1-encoded phosphatidate phosphatase isoforms. *J. Biol. Chem.* **285** 14628–14638

Han S, Bahmanyar S, Zhang P, Grishin N, Oegema K, Crooke R, Graham M, Reue K, Dixon JE and Goodman JM 2012 Nuclear envelope phosphatase 1-regulatory subunit 1 (formerly TMEM188) is the metazoan Spo7p ortholog and functions in the lipin activation pathway. *J. Biol. Chem.* **287** 3123–3137

Han GS, Siniossoglou S and Carman GM 2007 The cellular functions of the yeast lipin homolog Pah1p are dependent on its phosphatidate phosphatase activity. *J. Biol. Chem.* **282** 37026–37035

Han GS, Wu WI and Carman GM 2006 The Saccharomyces cerevisiae lipin homolog is a Mg^{2+}-dependent phosphatidate phosphatase enzyme. *J. Biol. Chem.* **281** 9210–9218

Horowitz S and Gorovsky MA 1985 An unusual genetic code in nuclear genes of Tetrahymena. *Proc. Natl. Acad. Sci. U. S. A.* **82** 2452–2455

Hsieh LS, Su WM, Han GS and Carman GM 2016 Phosphorylation of yeast Pah1 phosphatidate phosphatase by casein kinase II regulates its function in lipid metabolism. *J. Biol. Chem.* **291** 9974–9990

Johnson KR, Ellis G and Toothill C 1977 The sulfophosphovanillin reaction for serum lipids: a reappraisal. *Clin. Chem.* **23** 1669–1678

Karanasios E, Barbosa AD, Sembongi H, Mari M, Han GS, Reggiori F, Carman GM and Siniossoglou S 2013 Regulation of lipid droplet and membrane biogenesis by the acidic tail of the phosphatidate phosphatase Pah1p. *Mol. Biol. Cell* **24**, 2124–2133

Karanasios E, Han G, Xu Z, Carman GM and Siniossoglou S 2010 Aphosphorylation-regulated amphipathic helix controls the membrane translocation and function of the yeast phosphatidate phosphatase. *Proc. Natl. Acad. Sci. USA* **107** 17539–17544

Kim Y, Gentry MS, Harris TE, Wiley SE, Lawrence JC and Dixon JE 2007 A conserved phosphatase cascade that regulates nuclear membrane biogenesis. *Proc. Natl. Acad. Sci. USA* **104** 6596–6601

Knight JA, Anderson S and Rawle JM 1972 Chemical basis of the sulfo-phospho-vanillin reaction for estimating total serum lipids. *Clin. Chem.* **18** 199–202

Kohlwein SD 2010 Triacylglycerol homeostasis: insights from yeast. *J. Biol. Chem.* **285** 15663–15667

Mobberley PS, Sullivan JL, Angus SP, Kong X and Pennock DG 1999 New Axonemal Dynein Heavy Chains from *Tetrahymena thermophila*. *J. Euk. Microbiol.* **46** 147–154

Michot C *et al*. 2010 LPIN1 gene mutations: a major cause of severe rhabdomyolysis in early childhood. *Hum Mutat.* **31** 1564–1573

Nakamura Y, Koizumi R, Shui G, Shimojima M, Wenk MR, Ito T and Ohta H 2009 Arabidopsis lipins mediate eukaryotic pathway of lipid metabolism and cope critically with phosphate starvation. *Proc. Natl. Acad. Sci. USA* **106** 20978–20983

O'Hara L, Han G-S, Peak-Chew S, Grimsey N, Carman GM and Siniossoglou S 2006 Control of phospholipid synthesis by phosphorylation of the yeast lipin Pah1p/Smp2p Mg^{2+}-dependent phosphatidate phosphatase. *J. Biol. Chem.* **281** 34537–34548

Orias E, Cervantes MD and Hamilton EP 2011 *Tetrahymena thermophila*, a unicellular eukaryote with separate germline and somatic genomes. *Res Microbiol.* **162** 578–586

Orias E, Hamilton EP and Orias JD 2000 Tetrahymena as a laboratory organism: useful strains, cell culture, and cell line maintenance. *Methods Cell Biol.* **62** 189–211

Parfrey LW, Barbero E, Lasser E, Dunthorn M, Bhattacharya D, Patterson DJ and Katz LA 2006 Evaluating support for the current classification of eukaryotic diversity. *PLoS Genet.* **2** 2062–2073

Pascual F and Carman GM 2013 Phosphatidate phosphatase, a key regulator of lipid homeostasis. *Biochim. Biophys. Acta - Mol. Cell Biol. Lipids* **1831** 514–522

Phan J, Peterfy M and Reue K 2004 Lipin expression preceding peroxisome proliferator-activated receptor-c is critical for adipogenesis *in vivo* and *in vitro*. *J. Biol. Chem.* **279** 29558–29564

Pillai AN, Shukla S and Rahaman A 2017a An evolutionarily conserved phosphatidate phosphatase maintains lipid droplet

number and endoplasmic reticulum morphology but not nuclear morphology. *Biol. Open* **6** 1629–1643

Pillai AN, Shukla S, Gautam S and Rahaman A 2017b Small phosphatidate phosphatase (*TtPAH2*) of Tetrahymena complements respiratory function and not membrane biogenesis function of yeast PAH1. *J. Biosci.* **42** 613–621

Santos-Rosa H, Leung J, Grimsey N, Peak-Chew S and Siniossoglou S 2005 The yeast lipin Smp2 couples phospholipid biosynthesis to nuclear membrane growth. *EMBO J.* **24** 1931–1941

Sherman F 2002 Getting started with yeast contents. *Method. Enzymol.* **350** 3–41

Siniossoglou S 2009 Lipins, lipids and nuclear envelope structure. *Traffic* **10** 1181–1187

Siniossoglou S, Santos-rosa H, Rappsilber J, Mann M and Hurt E 1998 A novel complex of membrane proteins required for formation of a spherical nucleus. *EMBO J.* **17** 6449–6464

Su WM, Han GS and Carman GM 2014 Cross-talk phosphorylations by protein kinase C and Pho85p-Pho80p protein kinase regulate pah1p phosphatidate phosphatase abundance in saccharomyces cerevisiae. *J. Biol. Chem.* **289** 18818–18830

Su WM, Han GS, Casciano J and Carman GM 2012 Protein kinase A-mediated phosphorylation of Pah1p phosphatidate phosphatase functions in conjunction with the Pho85p-Pho80p and Cdc28p-Cyclin B kinases to regulate lipid synthesis in yeast. *J. Biol. Chem.* **287** 33364–33376

Turkewitz AP, Orias E and Kapler G 2002 Functional genomics: the coming of age for *Tetrahymena thermophila*. *Trends Genet.* **18** 35–40

Ugrankar R, Liu Y, Provaznik J, Schmitt S and Lehmann M 2011 Lipin is a central regulator of adipose tissue development and function in drosophila melanogaster. *Mol. Cell. Biol.* **31** 1646–1656

Zhang P and Reue K 2017 Lipin proteins and glycerolipid metabolism: Roles at the ER membrane and beyond. *Biochim. Biophys. Acta.* **1859** 1583–1595

Corresponding editor: B J RAO